ACS SENSORS

pubs.acs.org/acssensors

Article

Rapid Direct Detection of SARS-CoV-2 Aerosols in Exhaled Breath at the Point of Care

Dishit P. Ghumra,◆ Nishit Shetty,◆ Kevin R. McBrearty,◆ Joseph V. Puthussery, Benjamin J. Sumlin, Woodrow D. Gardiner, Brookelyn M. Doherty, Jordan P. Magrecki, David L. Brody, Thomas J. Esparza, Jane A. O'Halloran, Rachel M. Presti, Traci L. Bricker, Adrianus C. M. Boon, Carla M. Yuede,* John R. Cirrito,* and Rajan K. Chakrabarty*

Cite This: *ACS Sens.* 2023, 8, 3023−3031

Read Online

ACCESS | Metrics & More | Article Recommendations | Supporting Information

ABSTRACT: Airborne transmission via virus-laden aerosols is a dominant route for the transmission of respiratory diseases, including severe acute respiratory syndrome coronavirus 2 (SARS-CoV-2). Direct, non-invasive screening of respiratory virus aerosols in patients has been a long-standing technical challenge. Here, we introduce a point-of-care testing platform that directly detects SARS-CoV-2 aerosols in as little as two exhaled breaths of patients and provides results in under 60 s. It integrates a hand-held breath aerosol collector and a llama-derived, SARS-CoV-2 spike-protein specific nanobody bound to an ultrasensitive micro-immunoelectrode biosensor, which detects the oxidation of tyrosine amino acids present in SARS-CoV-2 viral particles. Laboratory and clinical trial results were within 20% of those obtained using standard testing methods. Importantly, the electrochemical biosensor directly detects the virus itself, as opposed to a surrogate or signature of the virus, and is sensitive to as little as 10 viral particles in a sample. Our platform holds the potential to be adapted for multiplexed detection of different respiratory viruses. It provides a rapid and non-invasive alternative to conventional viral diagnostics.

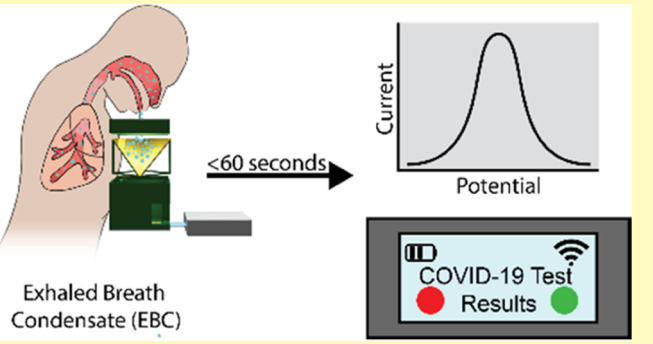

KEYWORDS: *aerosol science, virology, biosensors, electrochemistry, SARS-CoV-2*

Inhalation of virus-laden aerosols exhaled by infected individuals is deemed as a primary transmission mode of respiratory viruses such as severe acute respiratory syndrome coronavirus 2 (SARS-CoV-2),[1] influenza virus,[2] rhinovirus,[3] and respiratory syncytial virus (RSV).[4] Respiratory emissions during infection show the presence of viral RNA in a variety of aerosol sizes, with higher viral loads detected in aerosols <1 μm compared to larger-size aerosols.[5] Sub-micrometer sized virus aerosols are predominantly produced during breathing. The production of these aerosols involves bursting of the fluid film in respiratory bronchioles in the lower airways of a human lung.[6,7] In spite of the demonstrated significance of disease transmission via aerosols, techniques for direct, real-time detection of respiratory virus aerosols have remained elusive.

Screening non-invasively for SARS-CoV-2 viral RNA in breath aerosols remains a technical challenge (Table 1). The current state of research involves exhaled breath condensate (EBC) collection followed by reverse transcription-polymerase chain reaction (RT-PCR) to detect the prevalence of SARS-CoV-2 in various communities.[8] This methodology has limitations for mass testing applications due to long turnaround times and the need for sophisticated equipment and trained personnel. Electrochemical biosensors have previously been used for the detection of influenza[9−12] viruses (see Supporting Materials (SM) Table S2) and are rapidly emerging as an alternative to conventional clinical screening techniques. These sensing systems are simple, accurate, and possess a low limit of detection. However, most studies have demonstrated the use of electrochemical biosensors to detect SARS-CoV-2 in nasal swabs, saliva, or sputum samples.[13,14] Indirect methods of detection using electrochemical sensors have also been introduced to quantify the volatile organic compounds (VOCs)[15] in exhaled breath that are associated with COVID-19. These techniques discern a distinct pattern or signature of VOC emissions; thus, their feasibility might be hindered by the emergence of new SARS-CoV-2 variants. The situation

Received: March 17, 2023
Accepted: July 12, 2023
Published: July 27, 2023

Table 1. Summary of Studies on Detection of SARS-CoV-2 in Exhaled Breath Condensate (EBC)

sample collection technique	detection technique	sensitivity/detection rate (%)	point-of-care applications	limitations
exhaled breath condensate (EBC) using hand-held breathalyzer[16,17]	electrochemical sensor	100	yes	no description of device design or EBC collection volume
EBC using an R-Tube[16,18]	RT-PCR (target 1/4 genes)	31.3	no	low average detection rate
EBC using a R-Tube[19]	RT-PCR (various targets)	66.6−93.3	no	better for use in combination with NPS RT-PCR; no quantification of viral load
EBC using a turbo-DECC portable device[20]	RT-PCR	6	no	low detection rate; no quantification of viral load
EBC using a modified Inflammacheck device[21]	electrochemical sensor	92.3	yes	results are preliminary
exhaled breath using an electric filter-based device[22]	RT-qPCR	70	yes	highly variable viral load obtained in 100 specimens; detection rate low for EBC samples collected >5 days after diagnosis
exhaled breath using inspectIR COVID-19 breathalyzer (detection of 5 VOCs)[23]	rapid gas chromatography-mass spectrometry	91.2	yes	does not directly detect virus, presumptive diagnosis only; large equipment footprint
EBC using a hand-held breath sampler[24]	RT-qPCR	24.5	no	low detection rate and no quantification of viral load from EBC samples
EBC using a breath of health (BOH) analysis system[25]	Fourier-transform infrared (FTIR) spectroscopy with artificial intelligence (AI)	100	yes	detects signature of the virus; the emergence of new variants can hinder sensitivity
EBC using a disposable sampling device[26]	RT-qPCR test was realized on a silicon chip	∼74	yes	no quantification of viral load and low average detection rate
EBC using strip/pad affixed on a face covering[27]	colorimetric sensor using gold nanoparticles	100	yes	no SARS-CoV-2 positive patients tested; preliminary data is only based on ten COVID-negative subjects
EBC using an R-tube or R-tubeVent device[28]	RT-PCR after processing EBC samples through a nucleic acid purifier	∼25 (2/8 samples)	no	very preliminary results, larger cohort study needed to validate system
EBC using engineered breathing masks[29]	electrochemical aptasensor	71	yes	preliminary results and no quantification of viral load

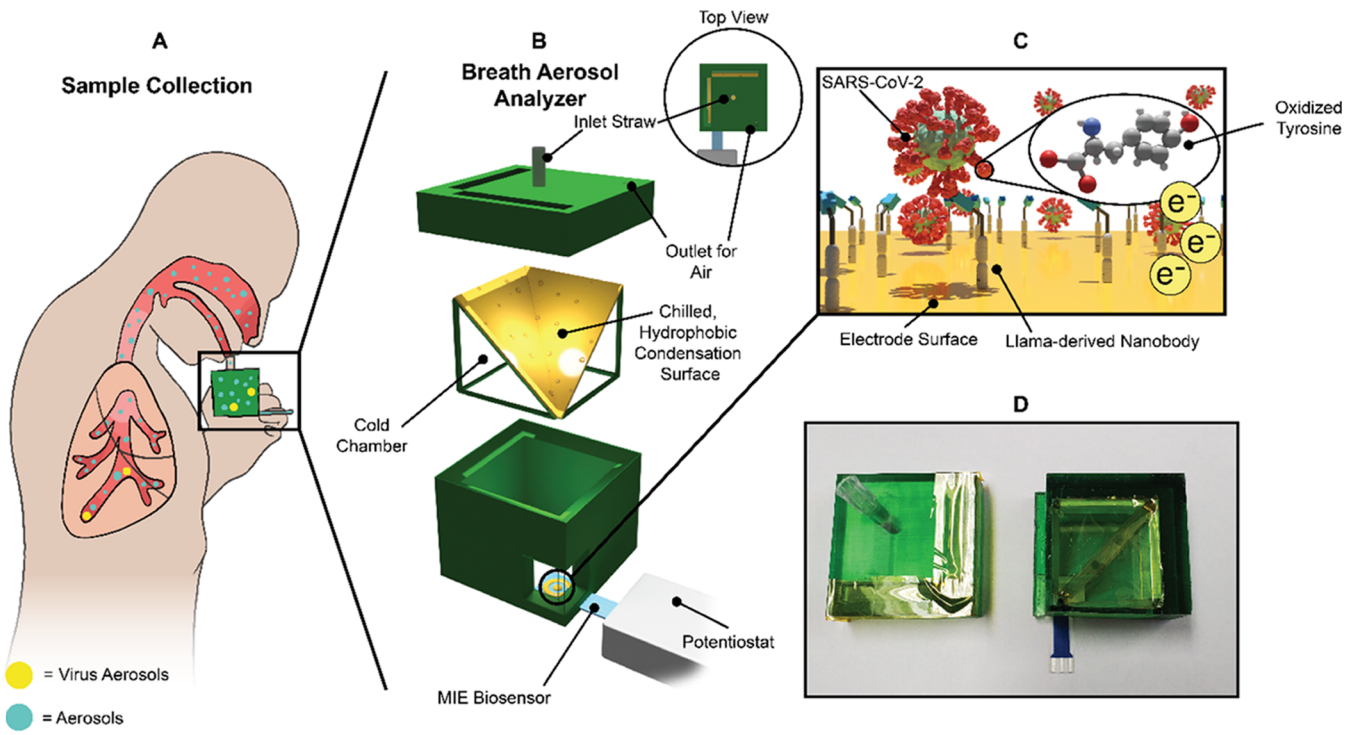

Figure 1. Illustration of SARS-CoV-2 detection using the Breath Aerosol Analyzer: (A) Sampling of the breath aerosols generated from the lower respiratory tract during normal breathing. (B) Schematic of the Breath Aerosol Analyzer system consisting of the aerosol collector, MIE biosensor, and a Potentiostat module. (C) Illustration of the mechanism of virus detection using the MIE biosensor. (D) Picture of the three-dimensional (3D)-printed breath aerosol collection box and the cap with an inlet straw.

underscores the need for variant-sensitive and rapid testing solutions at the point of need for early intervention and prevention of the community spread of the disease.

Here, we combine recent advances in EBC sampling and ultrasensitive electrochemical detection of SARS-CoV-2 variants using llama-derived nanobodies[30] to develop a hand-held, point-of-care breath aerosol analyzer with micro-immunoelec-

https://doi.org/10.1021/acssensors.3c00512
ACS Sens. 2023, 8, 3023−3031

trode (MIE) biosensor for clinical diagnosis. The breath aerosol collector has a detachable inlet straw through which a patient exhales into the device (Figure 1A,B). Virus-laden respiratory aerosols from the warm, exhaled breath impact and condense on the chilled hydrophobic surface. The surface is washed with 1 mL of 1% bovine serum albumin (BSA) in phosphate buffer saline (PBS) along the tapered incline to deliver the condensed aerosols to the bottom corner of the box, where the MIE biosensor is located. The biosensor uses screen-printed carbon-based electrodes with a nanobody originally derived in llamas covalently bound to the electrode surface to provide specificity to the SARS-CoV-2 spike protein.[31,32] The biosensor detects the oxidation of tyrosine amino acids present in the spike protein of SARS-CoV-2 (Figure 1C). The MIE biosensor is connected to a potentiostat (PalmSens, The Netherlands), and square-wave voltammetry is performed to oxidize tyrosine and measure the peak oxidation current corresponding to the presence of virus aerosols in a given sample. Tests will be single use and provide results in under 1 min, which is an improvement compared to conventional viral diagnostics.

In this study, we evaluate the performance of our novel breath aerosol analyzer, which combines an EBC method with SARS-CoV-2 detection using an ultrasensitive electrochemical biosensor. To test our device, we mimicked human breath by aerosolizing different SARS-CoV-2 variants in a laboratory setting. The sensitivity and specificity of the MIE biosensor were evaluated, and the limit of detection (LoD) was compared to typical viral RNA loads in exhaled breath to highlight the ultrasensitive nature of our biosensing system. We also present preliminary results from an ongoing clinical study evaluating the effectiveness of our device.

EXPERIMENTAL SECTION

Design of Testing Platform. The testing platform integrates a breath aerosol collection device and a MIE biosensor. The collection device (or box) has a cap with an inlet straw and two liquid injection ports (Figure 1B). It is 3D-printed using polylactic acid. The superhydrophobic surface in the collection device is inclined at 45° and enables the impaction and subsequent collection by condensation of aerosols from the exhaled breath. The surface may be of any suitable material, including but not limited to a hydrophobic film, or a film with a hydrophobic coating. Our breath aerosol collection device uses a polyimide film, which is coated with a thin layer of silicon wax to create an inclined hydrophobic surface. The aerosols from exhaled breath are gathered in a condensing chamber, which comprises the upper chamber of the box and consists of a tapered inclined hydrophobic polyimide condensing surface supported by a scaffold. The collection device is stored in a −20 °C freezer prior to running trials to cool the condensing surface. If a freezer is unavailable, a cold fluid like ice water can be added to the box's lower chamber through inlet points on the outer surface of the collection device.

When a person exhales into the device, the aerosols impact and condense on the chilled condensing surface, along with any viral particles that may be present. The surface is washed with 1 mL of 1% bovine serum albumin (BSA) in phosphate buffer saline (PBS) along the tapered inclined to deliver the condensed aerosols to the bottom corner of the box, where the MIE biosensor is located. Finally, after the EBC is analyzed by the biosensor, hypochlorous acid (HOCl) is injected through the second liquid injection port on the cap to sterilize the breathalyzer for its safe disposal.

The MIE biosensor uses inexpensive, screen-printed, carbon-based electrodes (SPiCE, Catalog# SP-1401, BASi Research Products, West Lafayette, IN). The core technology for the detection of SARS-CoV-2 virions from EBC is based on a micro-immunoelectrode (MIE) technology.[33,34] SPiCEs are pretreated in PBS (pH 7.4) and electro-activated to enhance selectivity for tyrosine oxidation and increase attachment of a SARS-CoV-2 specific nanobody. The nanobody is produced in llamas and is covalently attached to the electrode surface to concentrate the target at the MIE biosensor for measurement (Figure 1C). Importantly, tyrosine amino acids cannot be reduced to oxidize again, so any tyrosine present in the nanobody or BSA is oxidized in the electrode preparation and cannot provide a signal during the actual test.

During the prototype phase, the EBC samples were diluted in a cut glass vial containing 1% bovine serum albumin (BSA) in PBS solution rather than analyzed directly in the breath aerosol collection box. The MIE biosensor is connected to a commercial potentiostat, and square-wave voltammetry (SWV) is performed to oxidize tyrosines in the spike protein and detect current change at the electrode surface. In SWV, the current at the working electrode is measured while the electrode potential is scanned through 0−1 V using a frequency of 15 Hz. When the electroactive species is oxidized, a peak in oxidation current is observed in the voltammogram, which corresponds to the oxidation potential of that particular species. The presence of antibodies covalently attached to the electrode surface provides specificity to SARS-CoV-2 at a potential of 0.65 V.

While the breath collector is designed for single use as per USA FDA guidelines,[35,36] based on our lab characterization of the MIE Biosensor, a single biosensor can be reused for up to ∼70 sample scans. In the future, we will work toward building a reusable breath aerosol analyzer with in-built decontamination and cleaning mechanism.

Micro-Immunoelectrode (MIE) Biosensor—Binding of the Nanobody. In order to enhance tyrosine oxidation and efficient binding of the nanobody, the working electrodes are pretreated in PBS using a triangular waveform from 0 to 3 V at 70 Hz for 20 s, followed by holding at −0.8 and 1.5 V for 5 and 10 s, respectively. The activation of carboxylic groups on the electrode surface is achieved by using 0.4 M EDC (*N*-(3-dimethylaminopropyl)-*N*′-ethylcarbodiimide hydrochloride) and 0.1 M NHS (*N*-hydroxysuccinimide) solution (Thermo Scientific, IL) to form a semi-stable reactive amine NHS ester. The activated electrodes are placed in a solution of the nanobody and incubated for 10 min at room temperature, followed by 4 °C overnight. After the nanobody is attached to the electrode surface, the biosensors are incubated with 0.05% ethanolamine to deactivate the reactive amine sites and with 0.1% albumin to block non-specific protein binding sites. Importantly, tyrosine amino acids cannot be reduced to oxidize again, so any tyrosine present in the nanobody or BSA is oxidized in the electrode preparation and cannot provide a signal during the actual test.

Cells and Viruses. Dulbecco's Modified Eagle medium (DMEM) was used to culture the Vero cell line (37 °C) that expressed human ACE2 and TMPRSS2 (Vero-hACE2-hTMPRSS2, gift from Adrian Creanga and Barney Graham, NIH).[37,38] 10% fetal bovine serum (FBS), 10 mM HEPES (pH 7.3), 100 U/mL of Penicillin-Streptomycin, and 10 μg/mL of puromycin were added to this solution. Vero cells expressing TMPRSS2 (Vero-hTMPRSS2)[38] were cultured at 37 °C in Dulbecco's Modified Eagle medium (DMEM) combined with 10% FBS, 10 mM HEPES (pH 7.3), 100 U/mL of Penicillin-Streptomycin, and 5 μg/mL of blasticidin at a temperature of 37 °C.

The different SARS-CoV-2 variants were propagated on Vero-hTMPRSS2 cells. The infectious virus titer was determined by plaque assay on Vero-hACE2-hTMPRSS2 cells. In order to inactivate SARS-CoV-2, a culture supernatant containing infectious virus was treated for 18 h with 1:1000 dilution of β-Propiolactone (BPL). Plaque assay on Vero-hACE2-hTMPRSS2 cells confirmed the inactivation of SARS-CoV-2. A sample that was rendered inactive and a positive control were both included in the assay.[39]

Laboratory Aerosolization Experiments. We aerosolized inactivated SARS-CoV-2 variants in laboratory experiments. The experimental setup for the collection of EBC sample consists of the CHεST (CH Technologies Inc) and the breath aerosol analyzer (SM Figure S1). CHεST integrates a Blaustein Atomizing Module (BLAM, CH Technologies Inc.) that simulates the aerosol size distributions generated during various respiratory activities, such as breathing and sneezing. The cycle period and interval are set to 5 s each in order to simulate exhalation conditions.

https://doi.org/10.1021/acssensors.3c00512
ACS Sens. 2023, 8, 3023−3031

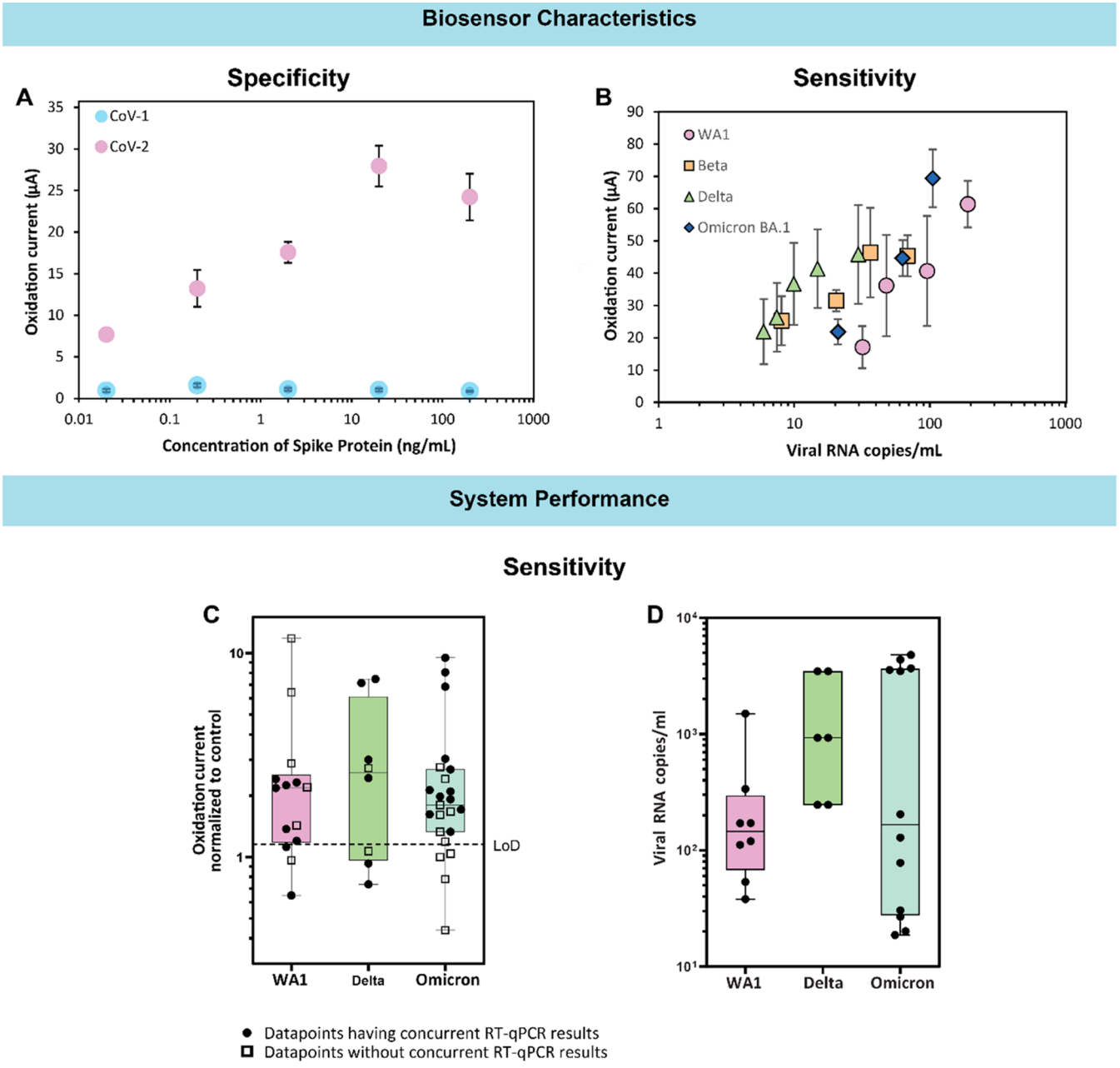

Figure 2. MIE Biosensor characteristics and EBC performance for SARS-CoV-2 detection: (A) Specificity of the MIE biosensor tested with SARS-CoV-1 and SARS-CoV-2 spike protein. (B) Biosensor sensitivity (or LoD) was evaluated by serial dilution of different SARS-CoV-2 variants. (C) Normalized oxidation current (I_{ox}) measured by the MIE biosensor in laboratory experiments. The horizontal dashed line denotes the limit of detection (LoD) of the system. (D) Viral RNA copies/mL determined using RT-qPCR for different aerosolized SARS-CoV-2 variants. The differences between viral RNA copies obtained for the three SARS-CoV-2 variants were statistically insignificant (*t*-test, $p = 0.17$) indicating that the strain of viruses did not impact the virus collection efficiency of the breath aerosol collection device. (*Whiskers denote the range of data, and the box represents the inter-quartile range).

We generated aerosols that mimic the size distribution of exhaled breath originating from the lower airways of the lungs,[6] and the volume of air nebulized corresponds to the expiratory volume from 10 to 15 "deep" breaths by a person. Hence, compressed air at a flow rate of 5.5 LPM (20 psi pressure setpoint) is sent to the CHεST and sample collection is done for a period of 10 min (SM Text S3). Additionally, the CHεST is paired with a syringe pump for efficient fluid delivery. Inactivated virus solution (100 μL of inactivated SARS-CoV-2 virus in 25 mL of PBS) is passed through the syringe pump to the BLAM at a flow rate of 0.9 mL/min. When the setup is switched on, the atomizer generates aerosols that travel to the breath aerosol collection device. There is a conical attachment with an extended cylindrical body that connects the outlet of the atomizer to the input straw of the collection device. It constricts the path of aerosols generated and results in greater impaction on the hydrophobic surface. At the end of the 10 min period, the surface is washed with 1 mL of 1% BSA in PBS solution, and the EBC sample is collected and sent for analysis by the MIE biosensor.

RT-qPCR. The viral load in EBC samples was quantified by RT-qPCR using a method similar to that of Darling et al.[39] The initial sample volume was 140 μL, and RNA extraction was carried out using QIAmp Viral RNA Mini Kit (Qiagen) as per the manufacturer's instructions and eluted with 60 μL of Buffer AVE. 8.5 μL of RNA was used for real-time RT-qPCR to detect and quantify the N gene of SARS-CoV-2 using the TaqMan RNA-to-CT 1-Step Kit (Thermo Fisher

https://doi.org/10.1021/acssensors.3c00512
ACS Sens. 2023, 8, 3023−3031

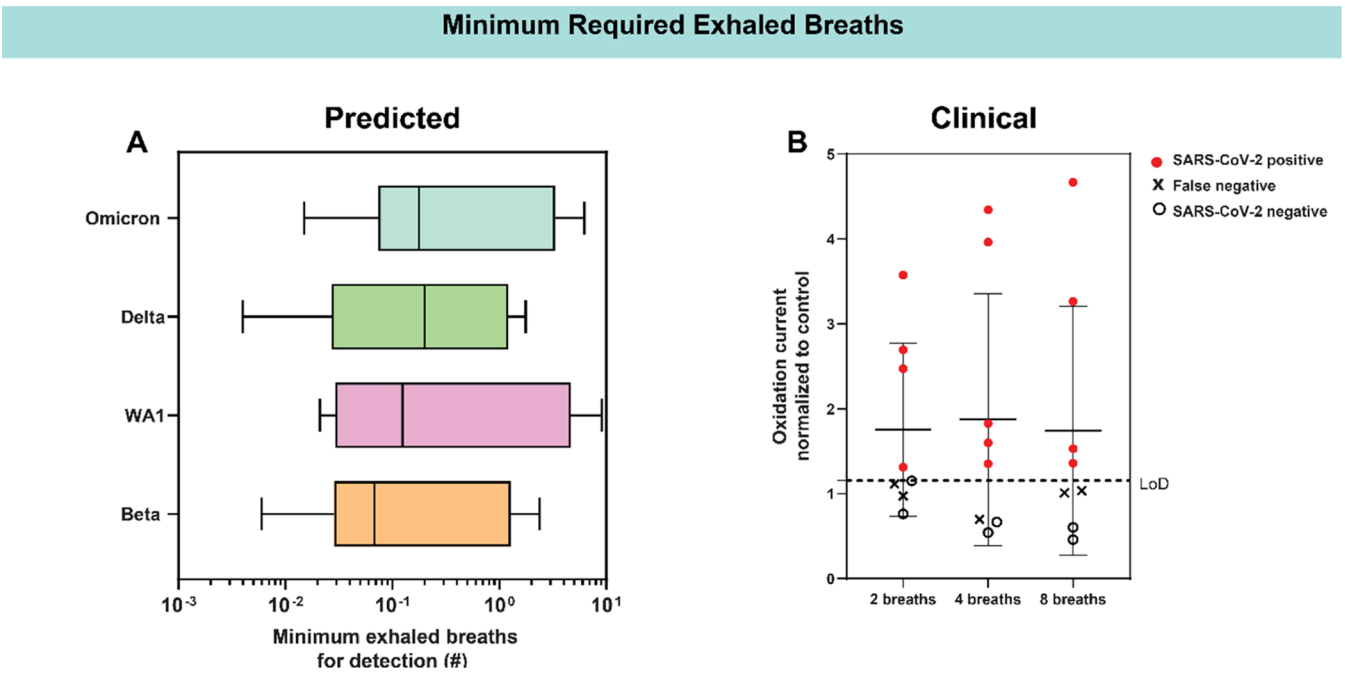

Figure 3. Estimating minimum number of exhaled breaths for detection by the MIE biosensor: (A) Number of exhaled breaths are predicted by evaluating the viral copies per breath for assumed range of viral load for COVID-19 patients. (B) Clinical study results demonstrate that SARS-CoV-2 viral particles are detected in as low as two exhaled breaths of patients.

Scientific) on a QuantStudio 12 K Flex Real-time Thermocycler (Applied Biosystems) using the default thermal cycling program. The probes and primers were used from the 2019-nCoV RUO kit (IDT). The viral load was expressed as N gene copy numbers per mL, based on a standard created by in vitro transcription of synthetic DNA molecules containing target regions of N gene. The primer efficacy was confirmed by analyzing the dissociation curves following the qPCR assay. Relative mRNA levels were calculated by the comparative Ct method using the ABI 12K Flex Software package version 1.3.

The Ct values were converted to $\log_{10}$ SARS-CoV-2 RNA copies/mL using a 5−9 point calibration curve of synthetic DNA molecules containing target regions of the N gene that is included in every RT-qPCR experiment (SM Figure S3). Ct values are calibrated on the five points surrounding the value of interest, which are typically the lowest five points. For nebulization studies, a negative control (aerosolized pure PBS solution) was processed in parallel to the test samples.

Clinical Study. In order to evaluate the performance of our diagnostic setup in human subjects, a clinical study is currently underway at the Infectious Disease Clinical Research Unit (IDCRU), Washington University School of Medicine (WUSM) with the approval of (institutional review board (IRB); approval number 202206152) (SM Text S2). We analyzed EBC samples from 8 participants (Six COVID positive and two COVID negative, as determined by RT-qPCR of nasopharyngeal swabs). For the clinical study, the design of the breath aerosol collection device is modified to include a slot at the bottom of the box that can fit an Eppendorf tube. Thus, the EBC sample can directly slide down the hydrophobic surface and is collected in the tube. The breath aerosol collection device is kept in a −20 °C freezer for at least 1 h prior to sample collection. Each participant blows into the breath aerosol collection device 2, 4, and 8 times. Thus, 3 samples are obtained from each participant. After sample collection is done, the collection unit is disinfected with HOCl and safely disposed. The EBC samples are then analyzed in the laboratory using the MIE biosensor for the presence of SARS-CoV-2.

RESULTS AND DISCUSSION

Platform Characterization and Performance. We tested the specificity of our MIE biosensor by comparing the peak tyrosine oxidation currents (I_{ox}) for varying concentrations of SARS-CoV-2 and SARS-CoV-1 spike proteins. SARS-CoV-2 produced a robust signal down to 20 pg of spike protein per mL of sample fluid and saturates around 20 ng/mL, whereas SARS-CoV-1 produced a negligible signal (Figure 2A). Our biosensor is highly specific toward SARS-CoV-2, despite both spike proteins having more than 70% of their genetic makeup in common.

We evaluated the limit of detection (LoD) of the MIE biosensor by sequential dilution of a purified inactivated SARS-CoV-2 stock solution and measuring the corresponding I_{ox} values for different virus concentrations (confirmed using RT-qPCR). The initial stock solution of the virus was diluted in series, and square-wave voltammetry was performed at each concentration (n = 5 scans) using five independent electrodes to test the reliability of the biosensor for each CoV-2 variant. The lowest virus RNA concentrations detected by the MIE biosensor were 32, 8, 6, and 21 RNA copies/mL for the USA/WAa1/2020 (WA1), β (B.1.351), Delta (B.1.617.2), and Omicron (BA.1) strains of SARS-CoV-2, respectively (Figure 2B). The biosensor LoD is equal to or better than comparable sensors in the literature.[40,41] Also, the LoD for all the variants is much lower than the typical viral RNA load in exhaled breath of individuals infected with SARS-CoV-2,[42,43] which highlights the potential of our MIE biosensor for ultrasensitive detection of virus aerosols in exhaled breath. An individual oxidized tyrosine releases two to four electrons that the MIE biosensor detects as current. The sensor response plateaus at higher concentrations for the β and Delta variants, likely a result of the Hook effect.[44]

To evaluate our device performance, we aerosolized inactivated SARS-CoV-2 virions of three different variants: WA1, Delta (B.1.617.2), and Omicron (BA.1) in laboratory experiments. We generated aerosols that mimic the size distribution of exhaled breath originating from the lower airways of lungs,[6] and the volume of air nebulized corresponds to the expiratory volume from 10 to 15 "deep" breaths by a person (SM Figures S1 and S2). Aerosolization runs using pure PBS solution

https://doi.org/10.1021/acssensors.3c00512
ACS Sens. 2023, 8, 3023−3031

constituted the control for our method. Figure 2C shows the average I_{ox} values measured for aerosolized virus sampled in the breath aerosol collector normalized to the I_{ox} values of the control, indicating a 77.8% sensitivity (n = 45) for this device. The sensitivity of our method is comparable to other electrochemical detection techniques for SARS-CoV-2;[41,45,46] however, our technique focuses on direct detection of virus-laden aerosols and will provide results in under 1 min.

The results from RT-qPCR determined that viral RNA for samples collected using the breath aerosol analyzer ranged from $10^{1.3}$ to $10^{3.7}$ gene copies/sample (Figure 2D). Our values are in line with viral loads reported using EBC-based methods,[43] which are approx. 3-4 orders lower in magnitude compared to that from nasal swabs,[22] and about 2−3 orders lower in magnitude in contrast to that from saliva samples.[47] COVID-19 infection results in 200−600 viral particles per breath,[42] which reinforces the feasibility of our method to detect virus aerosols in exhaled breath.

Clinical Validation. To validate the performance of our system in human patients, we employed our device in a clinical trial at the Infectious Disease Clinical Research Unit (IDCRU), Washington University School of Medicine (WUSM) with the approval of IRB (see SM Text S1). We analyzed EBC samples from 8 participants (six COVID positive and two COVID negative, as determined by RT-qPCR of nasopharyngeal swabs). We incorporated the effect of various parameters like typical viral loads in infected individuals, device collection efficiency, and LoD of the MIE biosensor to evaluate the number of breaths needed for sufficient sample collection to obtain satisfactory results using our device. As per Malik et al.,[22] the viral load in SARS-CoV-2 positive individuals ranges from 75-(3×10^4) copies/mL for 20 exhaled breaths in infected patients. This reference value enabled us to correlate viral load per exhaled breath and the biosensor LoD for different SARS-CoV-2 variants obtained through lab experiments. Based on the results obtained (see Figure 3A; see SM Text S2), we defined the sample collection protocol such that each participant blew into the collection device 2, 4, and 8 times with approx. 3 min between consecutive sample collection (n = 24 samples). The initial results (Figure 3B) denote a 77.9% sensitivity (n = 8 subjects) for our method, and a specificity of 100% as the analyte signal for both negative patients is below the LoD. The I_{ox} values also demonstrate that 2 exhaled breaths are sufficient for detection using our MIE biosensor. While the biosensor was tested with known inactivated viral particles in vitro through the BA.1 variant, the clinical study was conducted in St. Louis, Missouri in Summer to Fall 2022 when the BQ.1 variant was predominant, though the human subjects were not sequenced to determine which variant was present.

Concluding Remarks. In summary, we have demonstrated a portable, point-of-care testing platform integrating a novel breath aerosol collector and a nanobody-based MIE biosensor, costing less than 10 USD for each test, which will provide results in under 1 min. The sampling technique is non-invasive, and the detection method is rapid, facile, and does not warrant the need for highly trained personnel. Additionally, satisfactory results were obtained from just 20 s of sampling (2 exhaled breaths) compared to 5−30 min of sampling[16,18] in typical EBC-based studies. Finally, the MIE biosensor is highly sensitive for SARS-CoV-2 detection and has a lower LoD compared to similar devices reported in the literature.

The absolute value of tyrosine oxidation peak current measured (I_{ox}) using the biosensor depends on the amount of surface-attached nanobodies and the concentration of the analyte, along with extrinsic factors such as ambient relative humidity and temperature.[48] The variation in individual electrode responses precluded performing a direct comparison of gene copies obtained from RT-qPCR to the I_{ox} values. The consequences of the Hook effect[44] at higher viral loads needs further investigation.

Our platform is readily adaptable to not only detect different SARS-CoV-2 variants but also other respiratory pathogens of interest. Current efforts are underway for the simultaneous detection of multiple targets using distinct electrodes with different specific nanobodies. The initial results of our clinical study are quite promising; however, we need to validate the parameters reported here over a longitudinal clinical study to better analyze the effects of varying viral loads and disease comorbidities on the system performance.

■ ASSOCIATED CONTENT

Data Availability Statement

The data sets generated during the current study are available from the corresponding authors on written request.

Supporting Information

The Supporting Information is available free of charge at https://pubs.acs.org/doi/10.1021/acssensors.3c00512.

Lab experiment calculations and setup; breath aerosol analyzer manual of operations for clinical trial; calculations for predicted number of breaths and virus aerosol recovery (%) (PDF)

Illustration of the working mechanism of Breath Aerosol Analyzer for the detection of SARS-CoV-2 aerosols in exhaled breath (MP4)

■ AUTHOR INFORMATION

Corresponding Authors

Rajan K. Chakrabarty − *Center for Aerosol Science and Engineering, Department of Energy, Environmental and Chemical Engineering, Washington University in St. Louis, St. Louis, Missouri 63130, United States;* orcid.org/0000-0001-5753-9937; Email: chakrabarty@wustl.edu

John R. Cirrito − *Department of Neurology, Hope Center for Neurological Disease, Knight Alzheimer's Disease Research Center, Washington University, St. Louis, Missouri 63110, United States*; Email: cirritoj@wustl.edu

Carla M. Yuede − *Department of Psychiatry, Washington University School of Medicine, St. Louis, Missouri 63110, United States*; Email: yuedec@wustl.edu

Authors

Dishit P. Ghumra − *Center for Aerosol Science and Engineering, Department of Energy, Environmental and Chemical Engineering, Washington University in St. Louis, St. Louis, Missouri 63130, United States;* orcid.org/0000-0003-2480-3927

Nishit Shetty − *Center for Aerosol Science and Engineering, Department of Energy, Environmental and Chemical Engineering, Washington University in St. Louis, St. Louis, Missouri 63130, United States;* Present Address: Civil and Environmental Engineering, Virginia Tech, Blacksburg, Virginia 24061, USA

Kevin R. McBrearty − *Department of Neurology, Hope Center for Neurological Disease, Knight Alzheimer's Disease Research*

Center, Washington University, St. Louis, Missouri 63110, United States

Joseph V. Puthussery − *Center for Aerosol Science and Engineering, Department of Energy, Environmental and Chemical Engineering, Washington University in St. Louis, St. Louis, Missouri 63130, United States;* orcid.org/0000-0002-0185-1187

Benjamin J. Sumlin − *Center for Aerosol Science and Engineering, Department of Energy, Environmental and Chemical Engineering, Washington University in St. Louis, St. Louis, Missouri 63130, United States;* orcid.org/0000-0003-2909-7494

Woodrow D. Gardiner − *Department of Neurology, Hope Center for Neurological Disease, Knight Alzheimer's Disease Research Center, Washington University, St. Louis, Missouri 63110, United States*

Brookelyn M. Doherty − *Department of Neurology, Hope Center for Neurological Disease, Knight Alzheimer's Disease Research Center, Washington University, St. Louis, Missouri 63110, United States*

Jordan P. Magrecki − *Department of Neurology, Hope Center for Neurological Disease, Knight Alzheimer's Disease Research Center, Washington University, St. Louis, Missouri 63110, United States*

David L. Brody − *National Institute of Neurological Disorders and Stroke, Bethesda, Maryland 20892, United States; Department of Neurology, Uniformed Services University of the Health Sciences, Bethesda, Maryland 20814, United States*

Thomas J. Esparza − *National Institute of Neurological Disorders and Stroke, Bethesda, Maryland 20892, United States*

Jane A. O'Halloran − *Department of Medicine, Washington University, St. Louis, Missouri 63110, United States*

Rachel M. Presti − *Department of Medicine, Washington University, St. Louis, Missouri 63110, United States*

Traci L. Bricker − *Department of Medicine, Washington University, St. Louis, Missouri 63110, United States; Departments Molecular Microbiology, and Pathology and Immunology, Washington University School of Medicine, St. Louis, Missouri 63110, United States*

Adrianus C. M. Boon − *Department of Medicine, Washington University, St. Louis, Missouri 63110, United States; Departments Molecular Microbiology, and Pathology and Immunology, Washington University School of Medicine, St. Louis, Missouri 63110, United States;* orcid.org/0000-0002-4700-8224

Complete contact information is available at: https://pubs.acs.org/10.1021/acssensors.3c00512

Author Contributions

◆D.P.G., N.S. and K.R.M. contributed equally to this work. J.R.C., R.K.C., C.M.Y., and B.J.S. conceptualized research; D.P.G., N.J.S., K.M., J.V.P., B.J.S., W.D.G., B.M.D., J.P.M., T.J.E., and T.L.C. performed research and data analysis; and D.P.G, N.J.S., and R.K.C. wrote the paper with input from all authors.

Funding

This work was funded by the National Institutes of Health (NIH) RADx-Rad program under U01 AA029331 and U01 AA029331-S1 (J.R.C., R.K.C., and C.M.Y.), NIH, National Institute of Neurological Disorders and Stroke (NINDS) Intramural Research Program, and the Uniformed Services University of the Health Sciences (D.L.B.); NIH SARS-CoV-2 Assessment of Viral Evolution (SAVE) Program (A.C.M.B.) under 75N93021C00016.

Notes

The views expressed in this presentation are those of the authors and do not reflect the official policy or position of the Uniformed Services University, the U.S. Army, the Department of Defense, or the U.S. Government.

The authors declare the following competing financial interest(s): Y2X Life Sciences has an exclusive option to license the device technology and consulted during design stages of the device that may facilitate commercialization. A provisional patent covering NIH-CoVnb-112 and associated nanobody sequences was filed (U.S. Provisional Application No.: 63/055,865, Filing Date July 23, 2020) with a PCT patent application (application number PCT/US21/42883) filed on July 23, 2021 (D.L.B, T.J.E). All other authors declare that they have no competing interests.

A provisional patent covering NIH-CoVnb-112 and associated nanobody sequences was filed (U.S. Provisional Application No.: 63/055,865, Filing Date July 23, 2020) with a PCT patent application (application number PCT/US21/42883) filed on July 23, 2021 (D.L.B. and T.J.E). All other authors declare that they have no competing interests.

■ ACKNOWLEDGMENTS

The authors would like to thank the human subjects that participated in this clinical study, as well as the numerous staff at the Infectious Disease Clinical Research Unit (IDCRU) at Washington University School of Medicine who conducted the study. Y2X Life Sciences has an exclusive option to license the device technology and consulted during design stages of the device that may facilitate commercialization.

■ REFERENCES

(1) Wang, C. C.; Prather, K. A.; Sznitman, J.; Jimenez, J. L.; Lakdawala, S. S.; Tufekci, Z.; Marr, L. C. Airborne Transmission of Respiratory Viruses. *Science* **2021**, *373*, No. abd9149.

(2) Cowling, B. J.; Ip, D. K. M.; Fang, V. J.; Suntarattiwong, P.; Olsen, S. J.; Levy, J.; Uyeki, T. M.; Leung, G. M.; Peiris, J. S. M.; Chotpitayasunondh, T.; Nishiura, H.; Simmerman, J. M. Aerosol Transmission Is an Important Mode of Influenza A Virus Spread. *Nat. Commun.* **2013**, *4*, No. 1935.

(3) Fabian, P.; Brain, J.; Houseman, E. A.; Gern, J.; Milton, D. K. Origin of Exhaled Breath Particles from Healthy and Human Rhinovirus-Infected Subjects. *J. Aerosol Med. Pulm. Drug Delivery* **2011**, *24*, 137−147.

(4) Kulkarni, H.; Smith, C. M.; Do, D.; Lee, H.; Hirst, R. A.; Easton, A. J.; Callaghan, C. O. Evidence of Respiratory Syncytial Virus Spread by Aerosol Time to Revisit Infection Control Strategies? *Am. J. Respir. Crit. Care Med.* **2016**, *194*, 308−316.

(5) Robles-Romero, J. M.; Conde-Guillén, G.; Safont-Montes, J. C.; García-Padilla, F. M.; Romero-Martín, M. Behaviour of Aerosols and Their Role in the Transmission of SARS-CoV-2; a Scoping Review. *Rev. Med. Virol.* **2022**, *32*, No. e2297.

(6) Morawska, L.; Buonanno, G.; Mikszewski, A.; Stabile, L. The Physics of Respiratory Particle Generation, Fate in the Air, and Inhalation. *Nat. Rev. Phys.* **2022**, *4*, 723−734.

(7) Jarvis, M. C. Aerosol Transmission of SARS-CoV-2: Physical Principles and Implications. *Front. Public Health* **2020**, *8*, No. 590041.

(8) Nwanochie, E.; Linnes, J. C. Review of Non-Invasive Detection of SARS-CoV-2 and Other Respiratory Pathogens in Exhaled Breath Condensate. *J. Breath Res.* **2022**, *16*, No. 024002.

(9) Yang, Y. J.; Bai, Y. Y.; Huangfu, Y. Y.; Yang, X. Y.; Tian, Y. S.; Zhang, Z. L. Single-Nanoparticle Collision Electrochemistry Biosensor Based on an Electrocatalytic Strategy for Highly Sensitive and Specific

Detection of H7N9 Avian Influenza Virus. *Anal. Chem.* **2022**, *94*, 8392−8398.
(10) Dong, S.; Zhao, R.; Zhu, J.; Lu, X.; Li, Y.; Qiu, S.; Jia, L.; Jiao, X.; Song, S.; Fan, C.; Hao, R. Z.; Song, H. B. Electrochemical DNA Biosensor Based on a Tetrahedral Nanostructure Probe for the Detection of Avian Influenza A (H7N9) Virus. *ACS Appl. Mater. Interfaces* **2015**, *7*, 8834−8842.
(11) Bao, Q.; Li, G.; Yang, Z.; Liu, J.; Wang, H.; Pang, G.; Guo, Q.; Wei, J.; Cheng, W.; Lin, L. Electrochemical Biosensor Based on Antibody-Modified Au Nanoparticles for Rapid and Sensitive Analysis of Influenza A Virus. *Ionics* **2023**, *29*, 2021−2029.
(12) Devarakonda, S.; Singh, R.; Bhardwaj, J.; Jang, J. Cost-Effective and Handmade Paper-Based Immunosensing Device for Electrochemical Detection of Influenza Virus. *Sensors* **2017**, *17*, No. 2597.
(13) Samson, R.; Navale, G. R.; Dharne, M. S. Biosensors: Frontiers in Rapid Detection of COVID-19. *3 Biotech* **2020**, *10*, No. 385.
(14) Drobysh, M.; Ramanaviciene, A.; Viter, R.; Chen, C. F.; Samukaite-Bubniene, U.; Ratautaite, V.; Ramanavicius, A. Biosensors for the Determination of SARS-CoV-2 Virus and Diagnosis of COVID-19 Infection. *Int. J. Mol. Sci.* **2022**, *23*, No. 666.
(15) Abumeeiz, M.; Elliott, L.; Olla, P. The Use of Breath Analysis for Diagnosing COVID-19: Opportunities, Challenges, and Considerations for Future Pandemic Responses. *Disaster Med. Public Health Prep.* **2021**, 2137−2140.
(16) Giovannini, G.; Haick, H.; Garoli, D. Detecting COVID-19 from Breath: A Game Changer for a Big Challenge. *ACS Sens.* **2021**, *6*, 1408−1417.
(17) Shan, B.; Broza, Y. Y.; Li, W.; Wang, Y.; Wu, S.; Liu, Z.; Wang, J.; Gui, S.; Wang, L.; Zhang, Z.; Liu, W.; Zhou, S.; Jin, W.; Zhang, Q.; Hu, D.; Lin, L.; Zhang, Q.; Li, W.; Wang, J.; Liu, H.; Pan, Y.; Haick, H. Multiplexed Nanomaterial-Based Sensor Array for Detection of COVID-19 in Exhaled Breath. *ACS Nano* **2020**, *14*, 12125−12132.
(18) Sawano, M.; Takeshita, K.; Ohno, H.; Oka, H. RT-PCR Diagnosis of COVID-19 from Exhaled Breath Condensate: A Clinical Study. *J. Breath Res.* **2021**, *15*, No. 037103.
(19) Ryan, D. J.; Toomey, S.; Madden, S. F.; Casey, M.; Breathnach, O. S.; Morris, P. G.; Grogan, L.; Branagan, P.; Costello, R. W.; De Barra, E.; Hurley, K.; Gunaratnam, C.; Mcelvaney, N. G.; Obrien, M. E.; Sulaiman, I.; Morgan, R. K.; Hennessy, B. T. Use of Exhaled Breath Condensate (EBC) in the Diagnosis of SARS-COV-2 (COVID-19). *Thorax* **2021**, *76*, 86−88.
(20) Loconsole, D.; Paola, P.; Daniele, C.; Federica, B.; Maria, C.; Elisiana, C. G. Exhaled Breath Condensate (EBC) for SARS-CoV-2 Diagnosis Still an Open Debate. *J. Breath Res.* **2022**, *16*, No. 027101.
(21) Maniscalco, M.; Ambrosino, P.; Ciullo, A.; Fuschillo, S.; Valente, V.; Gaudiosi, C.; Paris, D.; Cobuccio, R.; Stefanelli, F.; Motta, A. A Rapid Antigen Detection Test to Diagnose Sars-Cov-2 Infection Using Exhaled Breath Condensate by a Modified Inflammacheck Device. *Sensors* **2021**, *21*, No. 5710.
(22) Malik, M.; Kunze, A. C.; Bahmer, T.; Herget-Rosenthal, S.; Kunze, T. SARS-CoV-2: Viral Loads of Exhaled Breath and Oronasopharyngeal Specimens in Hospitalized Patients with COVID-19. *Int. J. Infect. Dis.* **2021**, *110*, 105−110.
(23) Grob, N. M.; Aytekin, M.; Dweik, R. A. Biomarkers in Exhaled Breath Condensate: A Review of Collection, Processing and Analysis. *J. Breath Res.* **2008**, *2*, No. 037004.
(24) Kurver, L.; van den Kieboom, C. H.; Lanke, K.; Diavatopoulos, D. A.; Overheul, G. J.; Netea, M. G.; ten Oever, J.; van Crevel, R.; Mulders-Manders, K.; van de Veerdonk, F. L.; Wertheim, H.; Schouten, J.; Rahamat-Langendoen, J.; van Rij, R. P.; Bousema, T.; van Laarhoven, A.; de Jonge, M. I. SARS-CoV-2 RNA in Exhaled Air of Hospitalized COVID-19 Patients. *Sci. Rep.* **2022**, *12*, No. 8991.
(25) Shlomo, I. B.; Frankenthal, H.; Laor, A.; Greenhut, A. K. Detection of SARS-CoV-2 Infection by Exhaled Breath Spectral Analysis: Introducing a Ready-to-Use Point-of-Care Mass Screening Method. *eClinicalMedicine* **2022**, *45*, No. 101308.
(26) Stakenborg, T.; Raymenants, J.; Taher, A.; Marchal, E.; Verbruggen, B.; Roth, S.; Jones, B.; Yurt, A.; Duthoo, W.; Bombeke, K.; Fauvart, M.; Verplanken, J.; Wiederkehr, R. S.; Humbert, A.; Dang, C.; Vlassaks, E.; Uribe, A. L. J.; Luo, Z.; Liu, C.; Zinoviev, K.; Labie, R.; Frederiks, A. D.; Saldien, J.; Covens, K.; Berden, P.; Schreurs, B.; Van Duppen, J.; Hanifa, R.; Beuscart, M.; Pham, V.; Emmen, E.; Dewagtere, A.; Lin, Z.; Peca, M.; El Jerrari, Y.; Nawghane, C.; Arnett, C.; Lambrechts, A.; Deshpande, P.; Lagrou, K.; De Munter, P.; André, E.; Van den Wijngaert, N.; Peumans, P. Molecular Detection of SARS-COV-2 in Exhaled Breath at the Point-of-Need. *Biosens. Bioelectron.* **2022**, *217*, No. 114663.
(27) Jin, Z.; Mantri, Y.; Retout, M.; Cheng, Y.; Zhou, J.; Jorns, A.; Fajtova, P.; Yim, W.; Moore, C.; Xu, M.; Creyer, M. N.; Borum, R. M.; Zhou, J.; Wu, Z.; He, T.; Penny, W. F.; O'Donoghue, A. J.; Jokerst, J. V. A Charge-Switchable Zwitterionic Peptide for Rapid Detection of SARS-CoV-2 Main Protease. *Angew. Chem., Int. Ed.* **2022**, *61*, No. e202112995.
(28) Sawano, M.; Takeshita, K.; Ohno, H.; Oka, H. A Short Perspective on a COVID-19 Clinical Study: "Diagnosis of COVID-19 by RT-PCR Using Exhale Breath Condensate Samples. *J. Breath Res.* **2020**, *14*, No. 042003.
(29) Szunerits, S.; Dörfler, H.; Pagneux, Q.; Daniel, J.; Wadekar, S.; Woitrain, E.; Ladage, D.; Montaigne, D.; Boukherroub, R. Exhaled Breath Condensate as Bioanalyte: From Collection Considerations to Biomarker Sensing. *Anal. Bioanal. Chem.* **2023**, *415*, 27−34.
(30) Xu, J.; Xu, K.; Jung, S.; Conte, A.; Lieberman, J.; Muecksch, F.; Lorenzi, J. C. C.; Park, S.; Schmidt, F.; Wang, Z.; Huang, Y.; Luo, Y.; Nair, M. S.; Wang, P.; Schulz, J. E.; Tessarollo, L.; Bylund, T.; Chuang, G. Y.; Olia, A. S.; Stephens, T.; Teng, I. T.; Tsybovsky, Y.; Zhou, T.; Munster, V.; Ho, D. D.; Hatziioannou, T.; Bieniasz, P. D.; Nussenzweig, M. C.; Kwong, P. D.; Casellas, R. Nanobodies from Camelid Mice and Llamas Neutralize SARS-CoV-2 Variants. *Nature* **2021**, *595*, 278−282.
(31) Esparza, T. J.; Martin, N. P.; Anderson, G. P.; Goldman, E. R.; Brody, D. L. High Affinity Nanobodies Block SARS-CoV-2 Spike Receptor Binding Domain Interaction with Human Angiotensin Converting Enzyme. *Sci. Rep.* **2020**, *10*, No. 22370.
(32) Esparza, T. J.; Chen, Y.; Martin, N. P.; Bielefeldt-Ohmann, H.; Bowen, R. A.; Tolbert, W. D.; Pazgier, M.; Brody, D. L. Nebulized Delivery of a Broadly Neutralizing SARS-CoV-2 RBD-Specific Nanobody Prevents Clinical, Virological, and Pathological Disease in a Syrian Hamster Model of COVID-19. *mAbs* **2022**, *14*, No. 2047144.
(33) Yuede, C. M.; Lee, H.; Restivo, J. L.; Davis, T. A.; Hettinger, J. C.; Wallace, C. E.; Young, K. L.; Hayne, M. R.; Bu, G.; Li, C.-z.; Cirrito, J. R. Rapid in Vivo Measurement of SS-Amyloid Reveals Biphasic Clearance Kinetics in an Alzheimer's Mouse Model. *J. Exp. Med.* **2016**, *213*, 677−685.
(34) Prabhulkar, S.; Piatyszek, R.; Cirrito, J. R.; Wu, Z. Z.; Li, C. Z. Microbiosensor for Alzheimer's Disease Diagnostics: Detection of Amyloid Beta Biomarkers. *J. Neurochem.* **2012**, *122*, 374−381.
(35) FDA. Emergency Use Authorization of Medical Products and Related Authorities Guidance for Industry and Other Stakeholders; 2017.
(36) FDA. Policy for Coronavirus Disease-2019. 2020, pp 1−15.
(37) Chen, R. E.; Zhang, X.; Case, J. B.; Winkler, E. S.; Liu, Y.; VanBlargan, L. A.; Liu, J.; Errico, J. M.; Xie, X.; Suryadevara, N.; Gilchuk, P.; Zost, S. J.; Tahan, S.; Droit, L.; Turner, J. S.; Kim, W.; Schmitz, A. J.; Thapa, M.; Wang, D.; Boon, A. C. M.; Presti, R. M.; O'Halloran, J. A.; Kim, A. H. J.; Deepak, P.; Pinto, D.; Fremont, D. H.; Crowe, J. E.; Corti, D.; Virgin, H. W.; Ellebedy, A. H.; Shi, P. Y.; Diamond, M. S. Resistance of SARS-CoV-2 Variants to Neutralization by Monoclonal and Serum-Derived Polyclonal Antibodies. *Nat. Med.* **2021**, *27*, 717−726.
(38) Zang, R.; Castro, M. F. G.; McCune, B. T.; Zeng, Q.; Rothlauf, P. W.; Sonnek, N. M.; Liu, Z.; Brulois, K. F.; Wang, X.; Greenberg, H. B.; Diamond, M. S.; Ciorba, M. A.; Whelan, S. P. J.; Ding, S.TMPRSS2 and TMPRSS4 Promote SARS-CoV-2 Infection of Human Small Intestinal Enterocytes *Sci. Immunol.* 2020; Vol. 5 47, eabc3582. DOI: 10.1126/sciimmunol.abc3582.
(39) Darling, T. L.; Ying, B.; Whitener, B.; VanBlargan, L. A.; Bricker, T. L.; Liang, C. Y.; Joshi, A.; Bamunuarachchi, G.; Seehra, K.; Schmitz, A. J.; Halfmann, P. J.; Kawaoka, Y.; Elbashir, S. M.; Edwards, D. K.; Thackray, L. B.; Diamond, M. S.; Boon, A. C. M. MRNA-1273 and

Ad26.COV2.S Vaccines Protect against the B.1.621 Variant of SARS-CoV-2. *Med* **2022**, *3*, 309−324.e6.
(40) Agarwal, D. K.; Nandwana, V.; Henrich, S. E.; Josyula, V. P. V. N.; Thaxton, C. S.; Qi, C.; Simons, L. M.; Hultquist, J. F.; Ozer, E. A.; Shekhawat, G. S.; Dravid, V. P. Highly Sensitive and Ultra-Rapid Antigen-Based Detection of SARS-CoV-2 Using Nanomechanical Sensor Platform. *Biosens. Bioelectron.* **2022**, *195*, No. 113647.
(41) Torres, M. D. T.; de Araujo, W. R.; de Lima, L. F.; Ferreira, A. L.; de la Fuente-Nunez, C. Low-Cost Biosensor for Rapid Detection of SARS-CoV-2 at the Point of Care. *Matter* **2021**, *4*, 2403−2416.
(42) Johnson, T. J.; Nishida, R. T.; Sonpar, A. P.; Lin, Y. C. J.; Watson, K. A.; Smith, S. W.; Conly, J. M.; Evans, D. H.; Olfert, J. S. Viral Load of SARS-CoV-2 in Droplets and Bioaerosols Directly Captured during Breathing, Speaking and Coughing. *Sci. Rep.* **2022**, *12*, No. 3484.
(43) Zheng, J.; Wang, Z.; Li, J.; Zhang, Y.; Jiang, L.; Fu, Y.; Jin, Y.; Cheng, H.; Li, J.; Chen, Z.; Tang, F.; Lu, B.; Li, L.; Zhang, X. High Amounts of SARS-CoV-2 in Aerosols Exhaled by Patients with Omicron Variant Infection. *J. Infect.* **2022**, *84*, e126−e128.
(44) Pemberton, R. M.; Hart, J. P.; Mottram, T. T. An Electrochemical Immunosensor for Milk Progesterone Using a Continuous Flow System. *Biosens. Bioelectron.* **2001**, *16*, 715−723.
(45) Zhao, H.; Liu, F.; Xie, W.; Zhou, T. C.; OuYang, J.; Jin, L.; Li, H.; Zhao, C. Y.; Zhang, L.; Wei, J.; Zhang, Y. P.; Li, C. P. Ultrasensitive Supersandwich-Type Electrochemical Sensor for SARS-CoV-2 from the Infected COVID-19 Patients Using a Smartphone. *Sens. Actuators, B* **2021**, *327*, No. 128899.
(46) Chaibun, T.; Puenpa, J.; Ngamdee, T.; Boonapatcharoen, N.; Athamanolap, P.; O'Mullane, A. P.; Vongpunsawad, S.; Poovorawan, Y.; Lee, S. Y.; Lertanantawong, B. Rapid Electrochemical Detection of Coronavirus SARS-CoV-2. *Nat. Commun.* **2021**, *12*, No. 802.
(47) Savela, E. S.; Winnett, A. V.; Romano, A. E.; Porter, M. K.; Shelby, N.; Akana, R.; Ji, J.; Cooper, M. M.; Schlenker, N. W.; Reyes, J. A.; Carter, A. M.; Barlow, J. T.; Tognazzini, C.; Feaster, M.; Goh, Y. Y.; Ismagilov, R. F. Quantitative SARS-CoV-2 Viral-Load Curves in Paired Saliva Samples and Nasal Swabs Inform Appropriate Respiratory Sampling Site and Analytical Test Sensitivity Required for Earliest Viral Detection. *J. Clin. Microbiol.* **2022**, *60*, No. e01785-21.
(48) Wei, P.; Ning, Z.; Ye, S.; Sun, L.; Yang, F.; Wong, K. C.; Westerdahl, D.; Louie, P. K. K. Impact Analysis of Temperature and Humidity Conditions on Electrochemical Sensor Response in Ambient Air Quality Monitoring. *Sensors* **2018**, *18*, No. 59.

https://doi.org/10.1021/acssensors.3c00512
ACS Sens. 2023, 8, 3023−3031